Electronic materials

The unstable thermoelectric effect in non-stoichiometric Cu$_2$Se during the non-equilibrium phase transition

Bartosz Trawiński[1,*] , Marcin Łapiński[1], and Bogusław Kusz[1]

[1] Faculty of Applied Physics and Mathematics, Institute of Nanotechnology and Materials Engineering, Gdańsk University of Technology, G. Narutowicza 11/12, 80-233 Gdańsk, Poland

## ABSTRACT

The superionic $\alpha \leftrightarrow \beta$ phase transition in Cu$_{1.96}$Se thermoelectric material is investigated by means of thermal analysis (DSC) and measurements of Seebeck coefficient and electrical conductivity. Results of the DSC measurements with 1–10 K/min heating and cooling rates show that the material is close to the equilibrium phase composition during the transformation. However, the kinetic limitation of the process exists, which is indicated by supercooling. At the beginning of the $\beta \rightarrow \alpha$ transition, the most significant kinetic delay was attributed to the nucleation of the α phase. During the phase transformation, the Seebeck coefficient was lower than in a stabilised material (measured with 0.1 K/min heating/cooling rate). During cooling, a decrease from 130 μV/K (in a stabilised measurement) to 7 μV/K (5 K/min cooling rate) was observed. The deviation from the expected values of the Seebeck coefficient was correlated with the difference between the actual and equilibrium phase compositions.

Springer

GRAPHICAL ABSTRACT
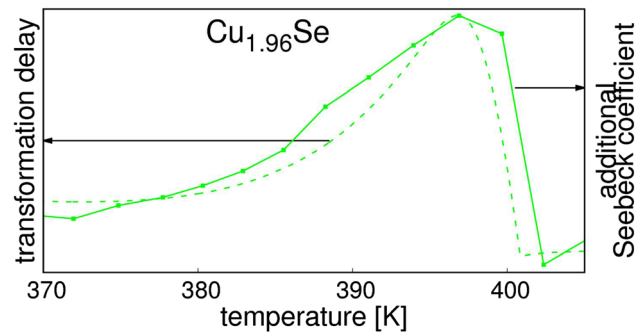
Introduction

Copper (I) selenide Cu_2Se is a well-known "thermoelectric material", that is a material with a strong thermoelectric effect. It is an analogue of Cu_2S, in which thermoelectricity is investigated since the early nineteenth century [1]. Copper selenide was investigated as a material for application in Peltier modules by NASA and 3M. These research works were dropped due to the instability of the material related to selenium volatility as well as the migration of copper, leading to the decomposition of the compound [2]. The latter issue has been recently addressed either by doping, e.g. [3, 4], leading to a decreased mobility of Cu^+ ions or decreasing the applied voltage, preventing the formation of metallic Cu phase [5]. Since 2012, copper selenide regained researchers' interest in the field of electricity [1]. One of the investigated issues is the superionic phase transition occurring in copper selenide. In the low-temperature α phase, Cu^+ ions are ordered within an FCC selenium sublattice, resulting in a hexagonal structure [6, 7]. The ordering of copper ions in crystallographic positions is not yet resolved. Some models of this phase were proposed, e.g. [6, 8, 9]. The coexistence of different structures is possible due to low differences in their energy [9]. Changes of the Cu ordering below the phase transition were found with three different low-temperature phases [10]. During the transition to the β structure, the ions form disordered "ionic liquid". The structure of the material becomes cubic, inherited from the Se sublattice. The liquid-like behaviour of copper causes strong phonon scattering and, consequently, low thermal conductivity, beneficial for thermoelectric applications. The material becomes superionic, with the conductivity of Cu + ions as high as 2.5 S/cm at 623 K [11].

The phase transition of copper selenide remains not fully understood. In the case of stoichiometric material, the transformation occurs, according to phase diagrams, at the temperature of 410 K. For non-stoichiometric $Cu_{2-\delta}Se$ (δ can vary between 0 and 0.22) [12], a mixture of α and β phases exists and the equilibrium ratio of the two phases changes with temperature. Moreover, mass transfer is involved due to δ values changing in these phases, according to the lever rule [13]. The phase transition manifests itself by a dispersed (λ-shaped) peak on DSC curves. The area of this maximum corresponds to about 6.3 kJ/mol (30 J/g) of heat energy [14–16]. Observed changes in phase composition (XRD patterns) and material's properties are also continuous. Some authors claim it to be a first-order phase transition, distributed along with temperature [14]. X-ray diffraction study of the transition [17] shows that the effect of coexistence of two phases is an intrinsic property of the material, which may be related to stoichiometry fluctuations. On the other hand, NMR spectroscopy results show a shift of a ^{63}Cu maximum rather than the presence of two spectrum peaks, expected for a two-phase system [18]. A recent study of crystal and band structure of Cu_2Se during the transition [7] shows an instantaneous change in the structure close to 400 K. This suggests that the observed coexistence of the two phases is related to

the small non-stoichiometry of the investigated samples. Moreover, a recent TEM study of the transformation of a single nanocrystal leads to a conclusion that the process is continuous rather than first order [19]. Whether the measured enthalpy is of a nature of latent heat or specific heat, its curves contribute to the thermal conductivity. This is a result of fast atom transferring between positions, on a time scale comparable with phonon scattering [13]. This is confirmed by measurements of the thermal conductivity with a Harman method [20].

An interesting feature of the phase transition is a giant Seebeck coefficient found in a particular temperature in the range of the transformation. A value of *c.a.* − 4000 µV/K was found [21]. Another recent report [22] shows the stability of this effect in time, with around − 1200 µV/K. These values are beyond the limits of a two-phase system determined by an effective medium theory [14]. A colossal change of the Seebeck coefficient close to the phase transition was also found in AgCuS [23]. DFT calculations show that, in AgCuS, it is related to a shift of the Fermi energy, which makes the material semi-metallic.

A study of the kinetics of the phase transition in Cu_2Se was published [15], with analysis based on DSC measurements. Kinetic curves obtained with different heating rates had similar onset and final temperatures, suggesting a small influence of kinetic barriers. This is in agreement with an autocatalytic mechanism model, related to "nucleus branching", which best fits to the data. The activation energy value of the phase transition process is about 1.8 eV. This result is inconsistent with the calculation results presented in [24]. The provided energy of different states of the reaction pathway should give an activation energy of *c.a.* 0.05 eV. Results presented in [15] are not compared with the properties of the material. No hysteresis was found in the XRD study of the transition [17]. However, no information on the heating and cooling rates was provided.

In this paper, we present the results of the thermal analysis of the phase transition in copper selenide. These results are correlated with measurements of the materials' thermoelectric properties performed with different heating rates. An influence of kinetic limitations of the transition on the Seebeck coefficient is observed.

Experimental

Cu_2Se was synthesised by a solid-state reaction of Cu (obtained by a reduction of CuO 99.99%) and Se (99.999%) in a fused silica ampule with low pressure of Ar. Powders were pressed into pellet with 350 MPa uniaxial pressure and heated up to 923 K with a 2 K/min heating rate. After 12 h, the sample was rapidly cooled. At this stage, Cu_2Se was already synthesised. In order to obtain homogeneity and high density, the material was hand-milled and pressed again, closed in the fused ampule and heated to 1448 K with a rate of 1 K/min and kept in this temperature for 6 h for melting. Then, it was cooled down to 973 K (1 K/min), annealed for 48 h and further cooled to room temperature with 1 K/min.

The structure of the obtained material was analysed with powder X-ray diffraction using Bruker D2 Phaser with CuKα radiation. For SEM imaging, FEI Quanta FEG 250 microscope with EDT secondary electrons detector was used. For elemental analysis, EDX spectroscopy was performed using the EDAX Genesis APEX 2i detector with the ApolloX SDD spectrometer. Spectrum analysis was performed with TEAM 5.0 software. Density was measured with a hydrostatic method. DSC curves were gathered with NETZSCH DSC 204 F1 Phoenix differential calorimeter in a nitrogen atmosphere. Mass of the investigated powder was about 5.6 mg. Five-min intervals were applied between the heating and cooling segments. Thermoelectric properties were measured using a Linseis LSR-4 device. The measured sample was rectangular with cross-section dimensions 1.5×2 mm and distance between sense electrodes 6 mm. For conductivity measurement, a 20-mA current was applied. For the measurement of the Seebeck coefficient, a temperature difference between sense electrodes of at least 0.9 K was used. The measurements were configured without waiting for temperature stabilisation. The heating and cooling rates given in the results below are effective values, including time for the temperature change between the measurement points and for measurement of the properties in each point. After switching from heating to cooling, the temperature difference changed rapidly. Measurements with different heating and cooling rates were done one after the other. Platinum Seebeck coefficient values from [25] were taken to obtain the absolute value of the sample's thermopower. Additionally, XPS spectroscopy was

performed on the sample after electrical measurements. Analysis was performed at room temperature under a pressure below 1.1×10^{-9} mBar. The photoelectrons were excited by an MgKα X-ray anode. An Omicron Argus hemispherical electron analyser with a round aperture of 4 mm was used. Measurements were taken in a constant analyser energy (CAE) mode with pass energy equal to 50 eV. To remove contaminations and oxides, the surface was etched with Ar ions before the measurement. The data were processed in CasaXPS.

To obtain information on the heat related to the phase transition, the DSC data (heat flow in mW/mg) were corrected for the Dulong–Petit heat capacity. Additionally, a linear background, calculated for the 416–453 K range, was subtracted from each measurement. The measured time and temperature data were used to calculate the actual heating rate at any given moment. Cu_2Se molar mass equal to 206.06 g/mol was used. The reaction rate was calculated, assuming that the total enthalpy of the transition is equal to 31.1 J/g. The value was taken from DSC measurements and is consistent with the literature data [14–16].

Results

The diffraction pattern of the investigated material is presented in Fig. 1. The diffraction peaks fit the Powder Diffraction File 47–1448 card, with data up to 80 degrees. No impurities were found. Moreover, the peak at 27.7°, characteristic for the β phase, was not found. The latter suggests that the material is close to
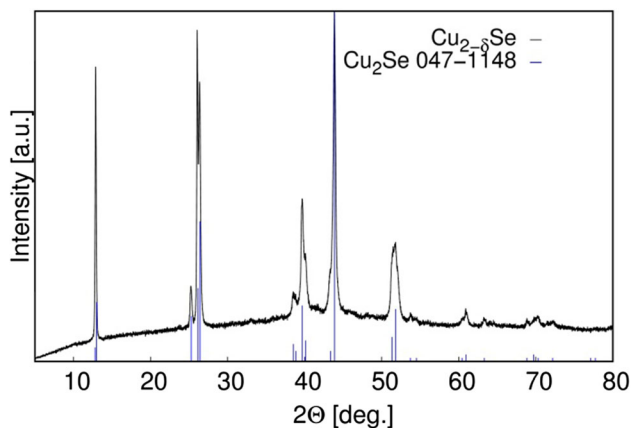
stoichiometric. SEM image is presented in Fig. 2. The material consists of grains with at least tens of micrometres in size. The fracture indicates a layered crystal structure of the material. Some pores are observed. The EDX elemental analysis returned a Cu:Se ratio equal to $(1.952 \pm 0.096):1$.

The reproducibility of the thermoelectric measurements was evaluated. Results presented in the Supplementary Material, Sect. 1, show that the first measurement cycle differs from the following, carried out directly after the first one. A similar effect was found in the In-doped Cu_2Se [3]. Therefore, the measurements analysed herein were preceded by an additional initial cycle.

Results of measurements of electrical conductivity and Seebeck coefficient are presented in Fig. 3. Heating and cooling rates were deviating from the programmed linear changes. For all measurements, the rates were constant at least in the 340–460 K range. Values provided in the plots are the actual heating/cooling rates calculated in the 340–460 K temperature range. Order of the cycles with different heating/cooling rates is given in the plots' key (cycle herein means one heating and cooling process). Measurements presented in Fig. 3 were taken immediately after the above-mentioned evaluation of the reproducibility of the results. We have observed that the results in the first thermal cycle (1 K/min) differ from those cycles that follow. Notice that the first cycle in Fig. 3 is reversible. (Initial and final properties are similar.) During the second cycle, the
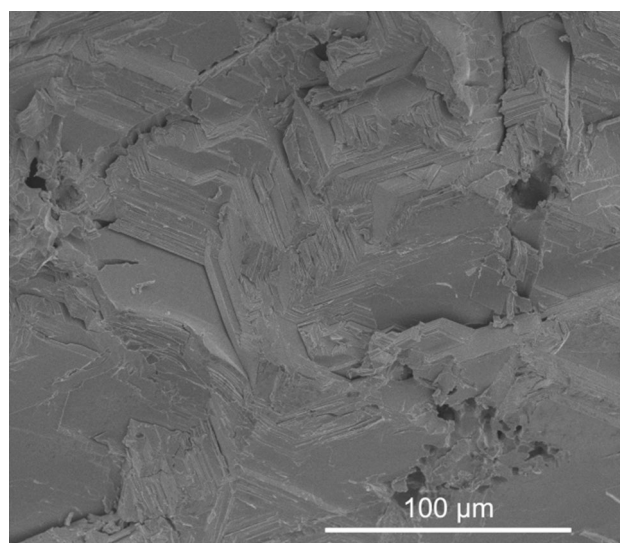

Figure 1 XRD pattern of the investigated material and peaks' positions of α-Cu_2Se in ICOD card 047–1448.

Figure 2 SEM image of the fraction surface of the investigated $Cu_{1.96}Se$.

Figure 3 Electrical conductivity **a**, **c** and Seebeck coefficient **b**, **d** values measured during heating **a**, **b** and cooling **c**, **d** in 5 successive thermal cycles. The order of the cycles is given by the key (top to bottom). Rates given in the key are actual measured values. In panel d, some Seebeck coefficient values above 408 K are deleted due to temperature difference below 0.9 K.
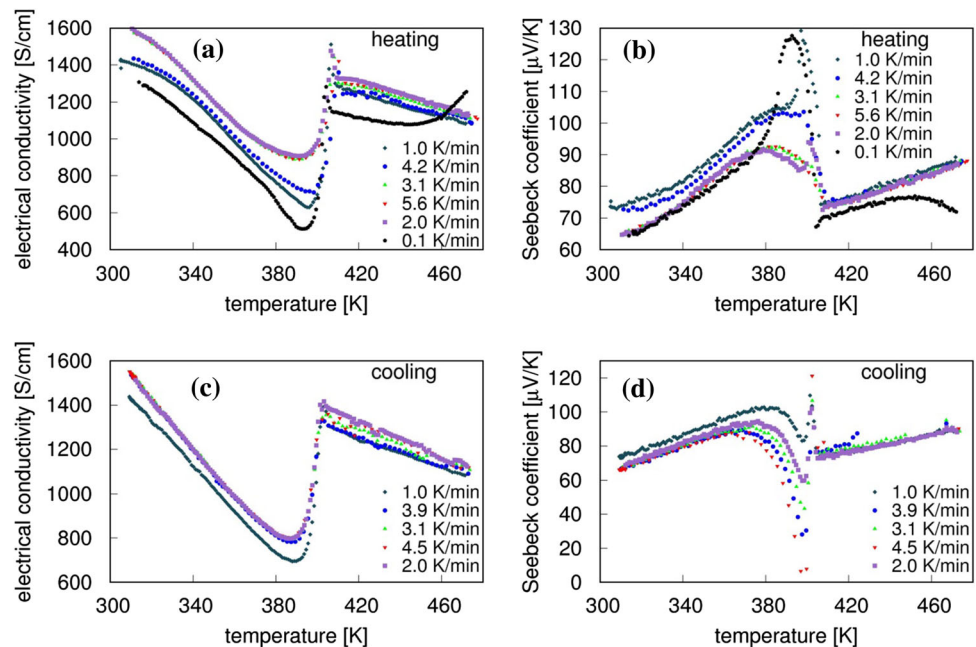
properties behave similarly to the first one during heating, whereas during cooling, the dependencies are close to the 3rd, 4th and 5th cycles, which are again reversible. Significant differences between heating and cooling can be noticed in the Seebeck coefficient values. In the cooling measurements, sharp positive and negative (in terms of direction) maxima are observed, similar to the colossal Seebeck coefficient effect [21, 22], despite not reaching mV/K values. Notice that values of the presented minima are correlated with the cooling rates.

After the runs with 1–5 K/min heating rates, an additional measurement with a 0.1 K/min heating rate was performed to measure the quasi-stable thermoelectric properties. Above *c a.* 440 K, the material was found to change its properties as a result of keeping at elevated temperatures for a long time. Increasing Seebeck coefficient and decreasing electrical conductivity were observed. This observation is in agreement with [26]. Therefore, only results obtained during the heating stage are presented in Fig. 3. This effect was not observed in the previous cycles because higher heating and cooling rates led to a shorter time of keeping the samples in elevated temperatures. The values measured during cooling with the 0.1 K/min rate cannot be directly compared to those presented in Fig. 3 and can be found in the Supplementary Material, Sect. 3.

Following these electrical measurements, additional EDX analysis and XPS spectroscopy were performed. The EDX returned a Cu:Se ratio equal to $(1.92 \pm 0.27):1$. Relevant regions of the XPS spectrum are provided in Supplementary Material, Fig. S5. The Se3d peak has a binding energy of 55.3 eV. This perfectly fits the zero-valent state of the element. The Cu2p maxima with binding energies 952.6 and 932.4 eV for $Cu2p_{1/2}$ and $Cu2p_{3/2}$, respectively, are characteristic for both metallic and $+ 1$ ionic copper. However, the peak at 917.5 eV for kinetic energy of the Cu L_3VV Auger electrons is characteristic of Cu^{1+} (in Cu_2O). No additional peak is observed for 918.6 eV, which would be characteristic of elemental Cu [27]. The Cu2p and Se3d positions are in agreement with previous studies [28, 29]. Auger electrons positions characteristic for the monovalent Cu are also typical for copper selenide [28]. The elemental composition calculated from the XPS spectrum is $Cu_{1.90}Se$, which is in line with EDX results.

Results of the DSC measurements are presented in Fig. 4a. The data are processed as described in Sect. 2. Measurements were taken in a 303–473 K temperature range. Results above the transition are not shown. In a low-temperature region, the actual heating and cooling rates were different from the programmed linear changes. For the deviation higher than 20%, the data were deleted. The phase composition of the sample was calculated, assuming that the total enthalpy of the transition is 31.1 J/g and that there is 100% of the β phase at 408 K. Furthermore, it was assumed that the heat is related to the "melting"
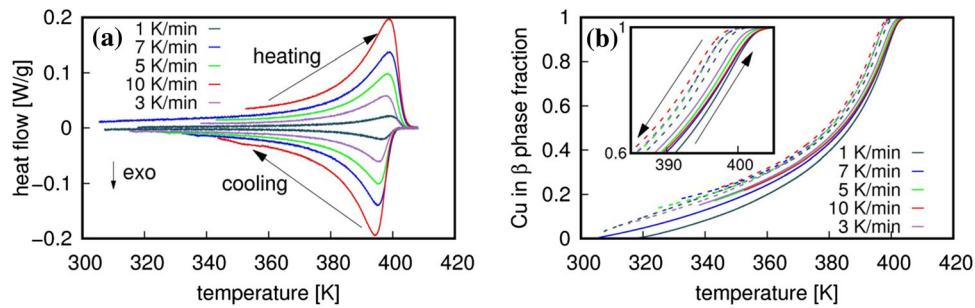
Figure 4 **a** DSC signal corrected for Dulong–Petit heat capacity and linear background measured during heating and cooling in different thermal cycles, limited to the analysed phase transition range; **b** fraction of copper in the β phase, calculated from the DSC data, solid lines represent heating segments, dashes lines—cooling. The order of the cycles is given by the key (top to bottom).

of Cu ions. Therefore, the progress of the $\alpha \to \beta$ transformation calculated from the DSC data is equal to the fraction of Cu atoms in the β phase. The calculated dependence of the β phase concentration on the temperature is presented in Fig. 4b. Notice that the transformation shows a hysteresis—the $\alpha \to \beta$ process during heating is shifted toward higher temperatures, than the opposite transformation during cooling. During cooling, the differences between the obtained temperature and transformation dependencies are correlated with the cooling rates. For the fastest rate, the highest "delay" is observed. However, results for 3, 5 and 7 K/min are similar. Interestingly, the deviations obtained for heating measurements are correlated with the rate of the corresponding rates of previous runs, e.g. the 3 K/min measurement was taken directly after the fastest one (with 10 K/min rate), and the corresponding curve is closest (on the temperature scale) to the curves obtained during cooling. The divergence between calculated dependencies in the low-temperature region may result from inaccurate background correction.

Discussion

The similarity between the thermoanalytical curves in heating and cooling processes (Fig. 4b) suggests that, at first approximation, the reaction can be considered in terms of thermodynamic equilibrium of the $\alpha \leftrightarrow \beta$ reversible transition, rather than the reaction kinetics. Following this conclusion, we have calculated the temperature dependence of the equilibrium fraction of copper in the high-temperature phase. The lever rule was applied to solvus lines from

the phase diagram given in [14]. For different values of Cu non-stoichiometry, different dependencies of phase composition on the temperature would be calculated. The non-stoichiometry value δ equal to 0.0416 was found to best match the experimental data. Notice that analysis of DSC data, compared to the known phase diagram, can be used to estimate the actual composition of the material. More details are available in Supplementary Material, Sect. 2. The selected non-stoichiometry value is within the uncertainty limit of the EDX results. The obtained dependence of the equilibrium reaction progress on the temperature is presented and compared with the thermal analysis results in Fig. 5. The similarity between processes performed with different cooling rates (3, 5, 7 K/min) is unexpected for the kinetically
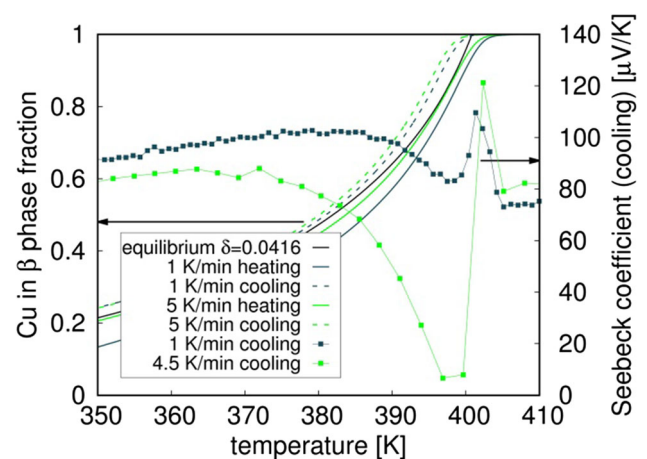

Figure 5 Equilibrium fraction of copper in the β phase, compared with values calculated from the selected DSC data measured during heating and cooling (solid and dashed lines), Seebeck coefficient measured during cooling with heating rates corresponding to the DSC measurements (points with lines).

controlled reactions; therefore, we chose only 1 and 5 K/min measurements for further analysis.

As can be noticed in Fig. 5, the concentration of the β phase is higher than that resulting from the phase diagram. Thus, the content of the emerging α phase during cooling is smaller than the equilibrium at any given temperature. Moreover, this difference between equilibrium and the measured progress of the transformation (vertical distance between the lines in Fig. 5) is related to the cooling rate. This suggests that there is a kinetic limitation of the speed of the process. In such processes, the transformations do not keep up with the changes in temperature (cannot be fast enough), and the delay becomes larger for the higher rate of temperature change. The observed transition is initially accelerating—does not have the highest reaction rate (proportional to the curve derivative) from the beginning, in contrast to the equilibrium curve. This may be related to a nucleation process. During heating, the material also was not following the equilibrium phase content. Correlation between deviation from the equilibrium and cooling rate of the previous thermal cycle indicated that not only the kinetic limitations but also an initial state, determined by the preceding cycle, influences the transformation. During the DSC thermal cycles, the lowest temperature reached was 305 K. For $\delta = 0.0416$, the β phase is still present in the material. Due to a small fraction of that phase, it was not detected in the XRD measurement.

The temperature dependence of the Seebeck coefficient measured during heating with a rate of 0.1 K/min is similar to the results published previously [20, 30] and matches calculations based on the Cu_2Se band structure measured with ARPES [7]. The positive maximum below 400 K results from changes in Cu mobility in the α phase [7]. Interestingly, it is visible here, despite the high-temperature β phase being the prominent one.

The results of the thermopower measurements with different heating rates will be discussed in terms of deviations from the quasi-stable measurement. When the temperature decreases, passing from β to $\alpha + \beta$ region of the phase diagram, the Seebeck coefficient initially increases, like in the quasi-stabilised measurement. However, the material does not further follow the equilibrium phase composition. Due to a nucleation-related delay and the fastest rate of the process expected from the phase diagram, the deviation of the phase composition rapidly increases.

Moreover, at the beginning of the transformation, the rate of the process expected from the phase diagram is fastest. At the same time, the thermopower rapidly becomes lower than in the 0.1 K/min quasi-stabilised measurement. The most prominent difference between the Seebeck coefficient values expected from the 0.1 K/min measurement and other runs is related to the sharp minimum below 400 K. Depth of this minimum (and the difference between measured and quasi-stable thermopower) is correlated with the cooling rate. This suggests that the deviation of the Seebeck coefficient may be related to the delay of the kinetically limited phase transition. Figure 3b shows that the Seebeck coefficient values obtained during heating also differ from the equilibrium curve. However, the DSC heating curves are more influenced by the cooling rate of the previous cycle rather than the heating rate.

The kinetic-dependent effect is observed only for the Seebeck coefficient. The electrical conductivity values are not dependent on the heating/cooling rate. At 345 K, the thermopower is strongly dependent on the chemical potential. This was found to be a reason for the colossal Seebeck coefficient observed at this temperature [21]. Here, the non-equilibrium conditions, caused by the kinetic limitations, may result in the actual non-stoichiometry values in both phases being different from those found on the phase diagrams. Consequently, the chemical potential changes. Thus, the measured values of the Seebeck coefficient can be attributed to chemical potential values not occurring under stable conditions.

The differences between the actual phase composition and the equilibrium one are presented in Fig. 6 together with corresponding differences in the Seebeck coefficient. The non-equilibrium thermoelectric effect correlates with the deviations from the expected equilibrium transition progress. The negative peak was not observed in measurements during heating, confirming smaller kinetic obstacles—the process is not limited by the nucleation close to the end of the transition in the heating direction.

It must be noted that the actual temperature difference between sense electrodes was changing between measurements. The higher the heating rate was, the lower the temperature difference was measured. In another experiment with a higher temperature difference (e.g. 4.5 K/min cooling rate with 3.2 K difference between electrodes, see Supplementary Material, Sect. 3), the temperature dependence of
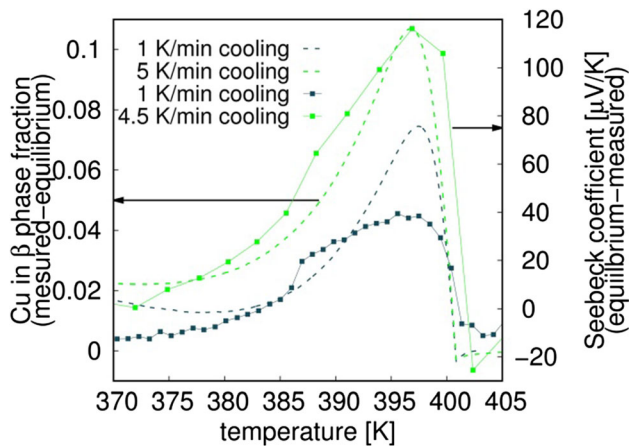
Figure 6 Differences between the progress of the phase transformation calculated from the DSC results and equilibrium based in the phase diagram (dashed lines); differences between Seebeck coefficient measured with cooling rates $\geq$ 1 K/min and quasi-equilibrium measured with the 0.1 K/min rate (points and solid lines).

Seebeck coefficient revealed a local minimum similar to the one, which occurred in the 2 K/min measurement (2.3 K temperature difference). Clearly, the investigated effect is influenced by the thermal gradient in the sample. It should be emphasised that the measured Seebeck coefficient values (presented herein) are actually average values of this property between the temperatures of sense electrodes. In case of any sharp features in the dependencies, taking average value will smooth the function. Notice that if the temperature gradient is small, the onset of the transformation is reached across the whole sample in a shorter time than when the temperature difference is higher. During cooling, the heat flow is the greatest close to the onset. Thus, the possible speed of heat release from the sample may be an additional external kinetic limitation of the phase transformation process, especially when the temperature gradient is small.

Conclusions

We have synthesised $Cu_{1.96}Se$ thermoelectric material. Despite taking stoichiometric amounts of the reactants, the analysis of the experimental data shows that the actual composition is close to $Cu_{1.96}Se$. The material was investigated in the range of the $\alpha \leftrightarrow \beta$ superionic phase transition using DSC analysis and measurement of electrical conductivity and Seebeck

coefficient. Heating and cooling rates equal to 1–10 K/min were applied for DSC measurements. 1–5 K/min rates were applied for thermoelectric properties measurements and 0.1 K/min to obtain reference, quasi-stable data.

Evaluation of the thermal analysis data shows that the $\alpha \leftrightarrow \beta$ phase transformation can be roughly described in terms of thermodynamic equilibrium, which is calculated based on the Cu–Se phase diagram. However, a more detailed analysis shows that during cooling, the material is not following the equilibrium concentration of the two phases. The magnitude of the deviation is correlated with the cooling rate, indicating a kinetically controlled process. The supercooling is most significant at the beginning of the $\beta \to \alpha$ transition, where the expected rate of the process is fastest. A delay related to nucleation may also be included. During heating, the kinetics are influenced by the initial state of the material—during consecutive thermal cycles performed, the fully-α state was not reached.

Interestingly, in our mixed-phase $(\alpha + \beta)$ non-stoichiometric system, the results of the quasi-stable measurement are similar to other published results of stoichiometric Cu_2Se samples without phase mixing. For higher heating and cooling rates, values of the Seebeck coefficient were found to be lower. In the cooling runs, a sharp minimum was observed on the temperature dependence of the Seebeck coefficient. The magnitude of this minimum was correlated with the cooling rate and with the scale of the supercooling. The latter indicates that the observed changes in the thermopower are related to the non-equilibrium phase composition.

The non-equilibrium effect presented herein takes place at the high-temperature edge of the phase transition. The measurement with a 0.1 K/min cooling rate shows that the phenomenon only occurs in dynamic conditions. In contrast, the effect discovered by Byeon [21] is at the low-temperature side and is stable [22] at a constant temperature.

Data availability

The research data used in this paper are available at The Bridge of Data repository, https://doi.org/10.34808/j5xa-6w81.

Declarations

Conflict of interest   There is no conflict of interest to declare.

References

[1] Dennler G, Chmielowski R, Jacob S et al (2014) Are binary copper sulfides/selenides really new and promising thermoelectric materials? Adv Energy Mater 4:1301581. https://doi.org/10.1002/aenm.201301581

[2] Brown DR, Day T, Caillat T, Snyder GJ (2013) Chemical stability of (Ag, Cu)2Se: a historical overview. J Electron Mater 42:2014–2019. https://doi.org/10.1007/s11664-013-2506-2

[3] Olvera AA, Moroz NA, Sahoo P et al (2017) Partial indium solubility induces chemical stability and colossal thermoelectric figure of merit in Cu2Se. Energy Environ Sci 10:1668–1676. https://doi.org/10.1039/C7EE01193H

[4] Kang SD, Pöhls J-H, Aydemir U et al (2017) Enhanced stability and thermoelectric figure-of-merit in copper selenide by lithium doping. Mater Today Phys 1:7–13. https://doi.org/10.1016/J.MTPHYS.2017.04.002

[5] Qiu P, Agne MT, Liu Y et al (2018) Suppression of atom motion and metal deposition in mixed ionic electronic conductors. Nat Commun 9:2910. https://doi.org/10.1038/s41467-018-05248-8

[6] Eikeland E, Blichfeld AB, Borup KA et al (2017) Crystal structure across the β to α phase transition in thermoelectric Cu$_{2-x}$Se. IUCrJ 4:476–485. https://doi.org/10.1107/S2052252517005553

[7] Sun S, Li Y, Chen Y et al (2020) Electronic origin of the enhanced thermoelectric efficiency of Cu2Se. Sci Bull 65:1888–1893. https://doi.org/10.1016/j.scib.2020.07.007

[8] Gulay L, Daszkiewicz M, Strok O, Pietraszko A (2011) Crystal structure of Cu2Se. Chem Met Alloy 4:200–205. https://doi.org/10.30970/cma4.0184

[9] Qiu W, Lu P, Yuan X et al (2016) Structure family and polymorphous phase transition in the compounds with soft sublattice: Cu2Se as an example. J Chem Phys 144:194502. https://doi.org/10.1063/1.4948609

[10] Lu P, Liu H, Yuan X et al (2015) Multiformity and fluctuation of Cu ordering in Cu$_2$Se thermoelectric materials. J Mater Chem A 3:6901–6908. https://doi.org/10.1039/C4TA07100J

[11] Balapanov MK, Yakshibaev RA, Mukhamed'yanov UK (2003) Ion transfer in solid solutions of Cu$_2$Se and Ag$_2$Se superionic conductors. Phys solid state 45(4):634–638. https://doi.org/10.1134/1.1568997

[12] Chakrabarti DJ, Laughlin DE (1981) The Cu-Se (Copper-Selenium) system. Bull Alloy Phase Diagr 2:305–315. https://doi.org/10.1007/BF02868284

[13] Agne MT, Voorhees PW, Snyder GJ (2019) Phase transformation contributions to heat capacity and impact on thermal diffusivity, thermal conductivity, and thermoelectric performance. Adv Mater 31:1–7. https://doi.org/10.1002/adma.201902980

[14] Kang SD, Danilkin SA, Aydemir U et al (2016) Apparent critical phenomena in the superionic phase transition of Cu$_{2-x}$Se. New J Phys 18:013024. https://doi.org/10.1088/1367-2630/18/1/013024

[15] Chrissafis K, Paraskevopoulos KM, Manolikas C (2006) Studying Cu2-xSe phase transformation through DSC

examination. J Therm Anal Calorim 84:195–199. https://doi.org/10.1007/s10973-005-7169-7

[16] Vasilevskiy D, Masut RA, Turenne S (2019) A phenomenological model of unconventional heat transport induced by phase transition in Cu 2–x Se. J Electron Mater 48:1883–1888. https://doi.org/10.1007/s11664-018-06856-2

[17] Tonejc A, Tonejc AM (1981) X-ray diffraction study on α ↔ β phase transition of Cu2Se. J Solid State Chem 39:259–261. https://doi.org/10.1016/0022-4596(81)90340-6

[18] Sirusi AA, Ballikaya S, Uher C, Ross JH (2015) Low-temperature structure and dynamics in Cu2Se. J Phys Chem C 119:20293–20298. https://doi.org/10.1021/acs.jpcc.5b06079

[19] Chen L, Liu J, Jiang C et al (2019) Nanoscale behavior and manipulation of the phase transition in single-crystal Cu2Se. Adv Mater 31:1804919. https://doi.org/10.1002/adma.201804919

[20] Vasilevskiy D, Keshavarz MK, Simard JM et al (2018) Assessing the thermal conductivity of Cu2−xSe alloys undergoing a phase transition via the simultaneous measurement of thermoelectric parameters by a Harman-based setup. J Electron Mater 47:3314–3319. https://doi.org/10.1007/s11664-017-6057-9

[21] Byeon D, Sobota R, Delime-Codrin K et al (2019) Discovery of colossal seebeck effect in metallic Cu2Se. Nat Commun 10:72. https://doi.org/10.1038/s41467-018-07877-5

[22] Byeon D, Sobota R, Singh S et al (2020) Long-term stability of the colossal seebeck effect in metallic Cu2Se. J Electron Mater 49:2855–2861. https://doi.org/10.1007/s11664-019-07884-2

[23] Guin SN, Pan J, Bhowmik A et al (2014) Temperature dependent reversible p–N–p type conduction switching with colossal change in thermopower of semiconducting AgCuS.

J Am Chem Soc 136:12712–12720. https://doi.org/10.1021/ja5059185

[24] Liu H, Yuan X, Lu P et al (2013) Ultrahigh thermoelectric performance by electron and phonon critical scattering in Cu2Se1-xIx. Adv Mater 25:6607–6612. https://doi.org/10.1002/adma.201302660

[25] Cusack N, Kendall P (1956) The absolute scale of thermoelectric power at high temperature. Proc Phys Soc 72:898–901. https://doi.org/10.1088/0370-1328/72/5/429

[26] Shi DL, Geng ZM, Shi L et al (2020) Thermal stability study of Cu1.97Se superionic thermoelectric materials. J Mater Chem C 8:10221–10228. https://doi.org/10.1039/d0tc01085e

[27] Wagner CD, Riggs WM, Davis LE, Moulder JF (1979) Handbook of X-Ray photoelectron spectroscopy. Perkin-Elmer Corporation, Eden Praire

[28] van der Putten D, Zanoni R (1995) From molecular copper-selenide clusters to bulk Cu2Se: evidence for hole-state localization obtained from XPS. Phys Lett A 208:351–355. https://doi.org/10.1016/0375-9601(95)00777-8

[29] Hamawandi B, Ballikaya S, Råsander M et al (2020) Composition tuning of nanostructured binary copper Selenides through rapid chemical synthesis and their thermoelectric property evaluation. Nanomaterials 10:854. https://doi.org/10.3390/nano10050854

[30] Brown DR, Day T, Borup KA et al (2013) Phase transition enhanced thermoelectric figure-of-merit in copper chalcogenides. APL Mater 1:052107. https://doi.org/10.1063/1.4827595

Publisher's Note Springer Nature remains neutral with regard to jurisdictional claims in published maps and institutional affiliations.